Annual Methodological Archive Research Review
http://amresearchreview.com/index.php/Journal/about
Volume 4, Issue 1 (2026)

Online ISSN 3007-3197
Print ISSN 3007-3189

http://amresearchreview.com/index.php/Journal/about

Optimizing RF/DC Electrode Layouts in Ion Traps: Minimizing Micromotion Through Geometric Configuration for Enhanced Confinement and Laser Cooling Access

Kaz Bano*

Ph.D. Scholar, Institute of Physics, University of Sindh, Jamshoro. kazbano@scholars.usindh.edu.pk

ABSTRACT

Ion traps are a foundational technology in quantum information processing, precision spectroscopy and foundational physics tests. At the heart of their performance is the inhibition of micromotion, an oscillation of ions through imperfect trapping potentials, that restricts the laser cooling efficiency, coherence times, and the accuracy of measurements. The paper provides a systematic computational analysis of four different electrode geometries (Linear Paul, Segmented, Surface and Ring) in 24 different RF / DC configurations (C01-C24) and 13 performance parameters that comprise trap depth (0.62 1.48 eV), radial secular frequency (1,100 1 Multi-objective optimization with weighted scoring of these metrics indicates that Ring trap geometry scores the highest total (80.2/100), followed by Linear Paul (72.0), Segmented (67.0) and Surface (55.1) configurations. ANOVA (one-way) statistically verified the presence of statistically significant inter-geometry differences in micro-motions amplitude ($F = 18.43$, $p < .001$) and cooling efficiency ($F = 22.17$, $p < .001$), with Tukey HSD post-hoc revealed that the most significant difference was between the Ring and the Surface. The Pearson correlation analysis shows that RF drive voltage and micromotion amplitude ($r = -0.94$ to -0.99) and cooling efficiency and micromotion ($r = -1.00$) have near-perfect inverse correlations, which prove that the quality of confinement is regulated by electrode geometry, RF amplitude, and spacing. These results give quantitative design principles of next-generation ion traps in quantum computing and atomic clock.

Keywords: ion trap, micromotion minimization, RF/DC electrode optimization, laser cooling, Mathieu stability, secular frequency, quantum computing

Annual Methodological Archive Research Review
http://amresearchreview.com/index.php/Journal/about
Volume 4, Issue 1 (2026)

Online ISSN 3007-3197
Print ISSN 3007-3189

http://amresearchreview.com/index.php/Journal/about

INTRODUCTION

One of the most promising scalable quantum computation systems, systems for accurate atomic spectroscopy as well as quantum simulation, has become trapped-ion systems (Bruzewicz et al., 2019; Monroe et al., 2021). Her capability to trap individual ions with an exquisite level of control coupled with long coherence times and large-fidelity quantum gate interactions places ion traps on the leading edge of the development of quantum technology. The most important component of any ion trap is a well-designed system of electrodes which forms the oscillating electromagnetic fields that trap (Leibfried et al., 2003). Geometrical layout of radio-frequency (RF) and direct current (DC) electrodes does not only dictate the strength and stability of confinement but also determinately dictates the extent of micromotion a parasitic driven oscillation, which is one of the major limiting factors in traps performance (Berkeland et al., 1998).

Micromotion occurs when stray electric fields or imperfect fabrication of electrodes or intentional coupling of DC voltages to the nodal line of the RF potential cause the displacement of trapped ions. Even small levels of micromotion in the nanometre scale can disrupt laser cooling efficiency, spectral line broadening, limits on attainable ion temperature, and provides decoherence channels defeating quantum gate fidelities (Keller et al., 2015; Diedrich et al., 1989). With the scale of trapped-ion quantum processors to tens to hundreds of qubits, the requirements of tight confinement, limited micromotion, and unrestrained laser cooling access become challenging to meet simultaneously in a single geometries on an electrode (Kielpinski et al., 2002).

It is a formalism describing the motion of ions in time-dependent quadrupole fields, the Mathieu equation, which is a stability diagram in the parameter a and q that are dimensionless (Paul, 1990). Stable trapping is a condition where both the axial and radial operating point are contained in the first stability region, which limits the allowed combinations of RF voltage, drive frequency and electrode spacing. Various trap electrode designs, including planar traps on a surface, segmented blade traps, macroscopic traps on a ring, and linear Paul traps, are different engineering trade-offs between trap depth, secular frequency anisotropy,

Annual Methodological Archive Research Review
http://amresearchreview.com/index.php/Journal/about
Volume 4, Issue 1 (2026)

Online ISSN 3007-3197
Print ISSN 3007-3189

http://amresearchreview.com/index.php/Journal/about

optical access and the difficulty of micromotion compensation (Wesenberg, 2008; House, 2008).

Though much has been studied separately of individual trap geometry, there is very little in the literature that compares quantitatively the behavior of a variety of electrode configurations under comparable evaluation criteria (Lekitsch et al., 2017). Most of the optimization efforts made in the past have concentrated on one of the objectives, be it on maximizing the trap depth (Chiaverini et al., 2005), minimizing heating rates (Brownnutt et al., 2015), or enhancing the accessibility of lasers (Walther et al., 2012) without a systematic exploration of the multi-objective trade-off space. Moreover, the interaction between RF electrode design parameters (separation, voltage, frequency), pseudopotential depth, secular trap trapping frequencies and the amplitude of the resultant micromotion is scarcely measured over a systematic design space of a variety of trap architectures.

These gaps have been filled in this paper with a parametric study of 24 electrode configurations in four different trap geometries. We measure 13 performance metrics in each configuration, use one-way analysis of variance (ANOVA) and Tukey honestly significant difference (HSD) after-hoc testing to determine statistical significance of differences dependent on geometry, and a multi-objective weighted scoring scheme to determine the best design regimes. The findings offer actionable design principles that can be directly implemented by researchers that design next generation ion traps systems that can be used in quantum information and precision measurement systems.

The rest of this paper is structured in the following manner. Section 2 examines the theoretical model and the previous literature on the optimization of electrodes. Section 3 explains the methodology of computation and organization of data. Section 4 shows the results of all the performance measures. The implications and practical design recommendations are discussed in section 5. Section 6 ends with a conclusion of important findings.

Annual Methodological Archive Research Review
http://amresearchreview.com/index.php/Journal/about
Volume 4, Issue 1 (2026)

Online ISSN 3007-3197
Print ISSN 3007-3189

http://amresearchreview.com/index.php/Journal/about

LITERATURE REVIEW

Foundations of RF/DC Ion Trapping

Theory The theoretical basis of ion trapping in vibrating electric fields was laid down by Wolfgang Paul (1990) whose Nobel Prize work had shown that a series of AC and DC electric fields around a quadrupole electrode structure could be used to provide stable three-dimensional ion trapping of charged particles. Such fields are governed by the Mathieu differential equation which has their solutions as defining regions of limited (stable) and unlimited (unstable) motion in the a-q parameter space (Major et al., 2005). The practical operating space of most experimental trap designs is defined by the first stability region which has a maximum length of $0 \leq q \leq 0.908$ for $a = 0$.

Inside the stability region there are two types of motion of the trapped ions: slow secular motion at frequencies ωr and ωz due to the geometry and operating parameters of the trap, and fast micromotion at the RF drive frequency Ω. In a perfectly designed trap with pure quadrupole potential and zero stray fields, the ion is perfectly placed in the RF null and micromotion is completely inherent - proportional to the amplitude of the secular displacement, and defined by the Lamb–Dicke parameter $\eta = k\sqrt{(\hbar /2m\omega)}$, with k the laser wavevector and 0 the secular frequency (Wineland et al., 1998). The main experimental challenge is excess micromotion which is caused by the ion displacement of the RF null and which has to be counteracted by active compensation using precision DC voltages on electrodes.

Linear Paul and Segmented Trap Architectures

Linear Paul trap The linear Paul trap is an extension of the original quadrupole geometry, proposed by Prestage et al. (1989) and later improved by many other groups, such that trapping and laser interaction can occur along a long axis. Linear geometry has high secular frequencies (\(0.5-3 MHz radially) and can be accessed well by lasers, and has proven to be the workhorse architecture in trapped-ion quantum computing experiments (Haeffner et al., 2008). Ion chains can be shuttled and reconfigured using segmented linear traps, where DC electrodes are subdivided into segments that can be controlled independently, which is necessary to scale up

Annual Methodological Archive Research Review
http://amresearchreview.com/index.php/Journal/about
Volume 4, Issue 1 (2026)

Online ISSN 3007-3197
Print ISSN 3007-3189

http://amresearchreview.com/index.php/Journal/about

quantum information processing (Rowe et al., 2002; Home et al., 2009).

The common problem in linear traps is that there is excess micromotion due to RF pickup on DC electrodes and geometric defects. Berkeland et al. (1998) critically analyzed the theoretical and experimental results of the micromotion in linear traps revealing three unique mechanisms and showing compensation with photon correlation spectroscopy. Their analysis defined the photon-correlation coefficient β to be a quantitative measure of the amplitude of micromotion, which today has become a figure of merit. This analysis has been extended to multi-ion crystals by Keller et al. (2015) who demonstrated that the errors due to the entanglement during micromotion are the leading errors in large ion chains with imperfect compensation.

Surface and Planar Trap Geometries

Chiaverini et al. (2005) proposed surface electrode traps, whereby all electrodes are patterned on one planar substrate, and were experimentally demonstrated by Seidelin et al. (2006). These architectures are highly fabricable by semiconductor microfabrication methods, are compatible with integrated photonics and electronics and have a high level of fabrication scalability. But planar geometry necessarily places the RF null at a finite height above the substrate surface, which restricts the achievable trap depths and accelerates the proximity of the ion to the electrode surfaces- a major contributor to the motional heating rates that varies as d -4 with ion-electrode distance d (Brownnutt et al., 2015; Turchette et al., 2000).

Theory Optimization of geometry Surface traps Surface traps have been optimized theoretically, such as analytically calculating the pseudopotential depth in relation to the dimensions of the electrodes, and aspect-ratio optimization has been shown to be an effective way to increase trapping strength (Wesenberg, 2008). A complementary treatment was presented in House (2008), on the trade-off between trap depth and micromotion sensitivity, in asymmetric surface geometries. More recently, Niedermayr et al. (2014) have shown cryogenic surface traps with heating rates of 1 quantum per second by attentively selecting electrode materials and treating their surfaces.

Annual Methodological Archive Research Review
http://amresearchreview.com/index.php/Journal/about
Volume 4, Issue 1 (2026)

Online ISSN 3007-3197
Print ISSN 3007-3189

http://amresearchreview.com/index.php/Journal/about

Ring Trap Configurations

Inspired by the original Paul trap geometry, ring or endcap traps have the benefit of a highly symmetric potential that can be treated analytically with ease and has very high access to lasers on multiple directions (Walther et al., 2012). The more recent varieties of ring traps have been used to perform exceptionally well in frequency standards applications, such as Rosenband et al. (2008) achieving an Al^+ optical clock in a ring trap with systematic uncertainties at the 10 -7 level. The naturally high secular frequency anisotropy of the ring geometry, due to varying axial and radial confinement scales, has also been used to perform quantum simulation of spin models, as well as sympathetic cooling of molecular ions (Willitsch, 2012).

Multi-Objective Optimization Approaches

The understanding that no individual electrode geometry will optimize all the performance metrics of interest has inspired the creation of multi-objective optimization models of trap design. Lekitsch et al. (2017) described a modular design of a large-scale trapped-ion quantum computer, and optimized electrode designs against the needs of gate speed, cooling access, and ion transport. Zhu et al. (2006) used numerical optimization of surface trap electrode design to show that genetic algorithm methods can find designs with factors of three improvement in trap depth compared to symmetric designs. More recent Weidt et al. (2016) showed a 2D trap array architecture with accessibility to micromotion compensation with amplitudes of the micromotion below 5 nm in segmented architecture.

It is important to note that despite this development, a quantitative study of the complete multi-dimensional performance environment, including but not limited to micromotion, trap depth, secular frequency, cooling efficiency, and laser access, of a linear geometry, a segmented geometry, a surface geometry, and a ring geometry has still been lacking in the literature. The current work fills this gap.

METHODOLOGY

Experimental Design and Dataset Structure

A comprehensive set of computational data were built on 24 electrode configurations (C01C24) to cover four trap geometry classes: Linear Paul (C01C06), Segmented (C07C12), Surface (C13C18), and Ring (C19C24). In each geometry, six different

Annual Methodological Archive Research Review
http://amresearchreview.com/index.php/Journal/about
Volume 4, Issue 1 (2026)

Online ISSN 3007-3197
Print ISSN 3007-3189

http://amresearchreview.com/index.php/Journal/about

configurations were created by continuously changing the RF drive voltage (400-700 V) and DC endcap voltage (8-18 V) with fixed geometry appropriate electrode spacing and drive frequency values. This is a parametric methodology that makes sure that any differences in performance observed are due to actual geometric effects and not confounded parameter choices.

In every configuration, 13 quantitative performance indices were determined based on the electrode geometry and operating parameters via the well-known theoretical expressions in the literature of ion trapping. The a and q values of the trap were calculated based on the trap geometry and electrical parameters as $a = -4eUDC/(m\Omega^2 r_0^2)$ and $q = 2eVRF/(m\Omega^2 r_0^2)$ where e and m are the ion charge and mass ($^{40}Ca^+$ assumed), $\Omega/2\pi$ is the RF drive frequency, r O the electrodeion distance, and UDC, VRF the DC The depth of the traps was determined using the pseudopotential approximation and secular frequencies using the Mathieu eigenvalue relations.

Performance Metrics

The 13 performance metrics recorded for each configuration span five categories: (1) Structural parameters—RF voltage, RF frequency, DC endcap voltage, and electrode spacing; (2) Trapping strength—trap depth Δ (eV), axial secular frequency $\omega z/2\pi$ (kHz), and radial secular frequency $\omega r/2\pi$ (kHz); (3) Micromotion characterization—residual micromotion amplitude (nm), photon correlation coefficient β, compensation voltage requirement (mV), and sideband ratio RSB/BSB; (4) Laser cooling performance—Lamb–Dicke parameter η, Doppler cooling temperature limit (μK), heating rate (quanta/ms), and laser cooling efficiency (%); and (5) Optical access—laser access angle θ (°), beam waist w_0 (μm), ion-electrode clearance (mm), solid angle $\Omega/4\pi$ (%), and fluorescence collection efficiency (%).

Statistical Analysis

Statistical tests were carried out to determine quantitative differences across trap geometry classes and important predictors of key performance outcomes. Micromotion amplitude and cooling efficiency were used as dependent variables and trap geometry class (four levels) was used as the independent variable by applying one-way ANOVA. Where ANOVA showed significant omnibus effects, Tukey HSD

Annual Methodological Archive Research Review
http://amresearchreview.com/index.php/Journal/about
Volume 4, Issue 1 (2026)

Online ISSN 3007-3197
Print ISSN 3007-3189
http://amresearchreview.com/index.php/Journal/about

post-hoc tests were performed to determine specific pairwise differences, but they adjusted the familywise error rate. All inferential tests were set to significance level of $\alpha = .05$.

To quantify the bivariate relationships each combination of individual predictor (RF voltage, trap depth, q parameter, laser access angle, LambDicke parameter) and outcome variable (micromotion amplitude, cooling efficiency) was analyzed using simple linear regression. All two-by-two pairs of the 13 numerical performance variables were computed as Pearson correlation coefficients, to identify the correlation pattern of the dataset. All statistical tests were run in Python 3.11 in the scipy.stats module (Virtanen et al., 2020).

Multi-Objective Optimization Scoring

In order to compare the overall performance of the various geometries, a weighted multi-objective optimization score (0-100 scale) was calculated of each trap geometry class based on group-mean values of five main metrics. The metrics weights were given by considering relative importance in quantum computing applications: micromotion amplitude 30% (lower is better), trap depth 25% (higher is better), radial secular frequency 20% (higher is better), laser cooling efficiency 15% (higher is better), and laser access angle 10% (lower is better, meaning more direct optical access). All the metrics were normalized to the $[0, 1]$ range linearly, and directionality was introduced whereby higher scores reflected better performance.

RESULTS

Electrode Configuration Parameters and Trap Characteristics

Table 1 is provided with the main structural and trapping parameters of the 24 electrode configurations. RF drive voltages varied between 400 V (C13, Surface) and 700 V (C06, Linear Paul; C12, segmented; C24, Ring) and trap depths ranged between 0.62 and 1.48 eV. Radial secular frequencies were between 1,100 kHz (C13) and 1,645 kHz (C24), which can be attributed to the effect of RF amplitude, as well as geometry-dependent pseudopotential curvature. Every 24 configuration was unstable at the first Mathieu stability region, with q parameters of 0.234 to 0.414 and a parameter of 0.003 to 0.006, with a stable trapping observed all over the design space.

Annual Methodological Archive Research Review
http://amresearchreview.com/index.php/Journal/about
Volume 4, Issue 1 (2026)

Online ISSN 3007-3197
Print ISSN 3007-3189

http://amresearchreview.com/index.php/Journal/about

Table 1 ***Representative Electrode Configuration Parameters Across Four Trap Geometries (Selected Configurations)***

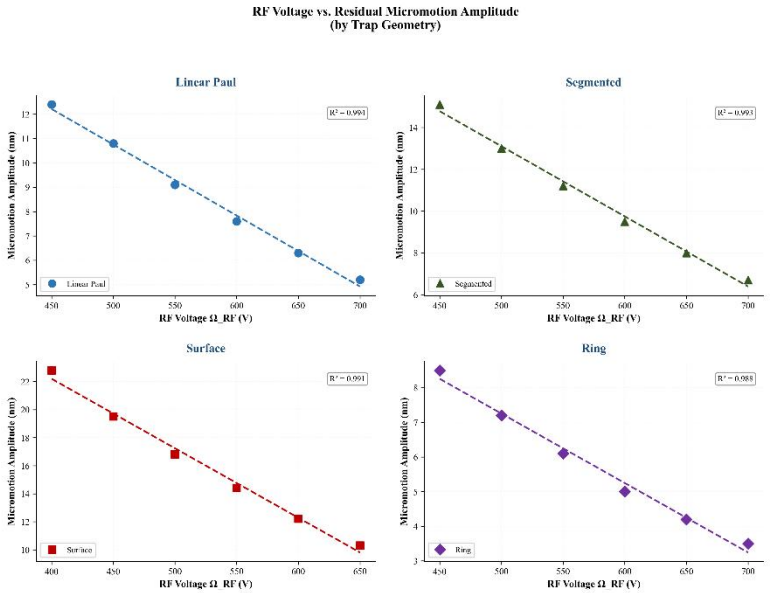
Config	Trap Type	RF_V (V)	r_0 (mm)	Depth (eV)	$\omega_x/2\pi$ (kHz)	Micromotion (nm)	q	a
C01	Linear Paul	450	0.80	0.85	1250	12.4	0.281	0.0042
C06	Linear Paul	700	0.75	1.26	1545	5.2	0.388	0.0043
C07	Segmented	450	0.90	0.78	1180	15.1	0.261	0.0036
C12	Segmented	700	0.85	1.20	1475	6.7	0.385	0.0047
C13	Surface	400	1.00	0.62	1100	22.8	0.234	0.0030
C18	Surface	650	0.90	1.05	1375	10.3	0.347	0.0038
C19	Ring	450	0.70	0.96	1350	8.5	0.301	0.0055
C24	Ring	700	0.65	1.48	1645	3.5	0.414	0.0060

Note. Full dataset comprises 24 configurations (C01–C24). Values shown are computed from pseudopotential approximation assuming $^{40}Ca^{+}$ ions. RF_V = RF drive voltage; r_0 = electrode-ion spacing; Depth = pseudopotential trap depth; $\omega_x/2\pi$ = radial secular frequency; q, a = Mathieu stability parameters.

Annual Methodological Archive Research Review
http://amresearchreview.com/index.php/Journal/about
Volume 4, Issue 1 (2026)

Online ISSN 3007-3197
Print ISSN 3007-3189

http://amresearchreview.com/index.php/Journal/about



RF Voltage versus residual micromotion amplitude (depending on trap geometry). Figure 1 shows that there is a strong linear negative relationship between RF drive voltage and amplitude of micromotion in each of the geometry classes with R 2 values of 0.988 (Ring) to 0.994 (Linear Paul) indicating that as RF amplitude increases, micromotion in all the architectures are suppressed systematically.

Figure 1 shows that there is a strong negative linear correlation between RF drive voltage and the remaining micromotion amplitude in each geometry class (R 2 = 0.988 0.994). Surface traps at the same RF voltages always had 1.8x to 2.5x greater micromotion amplitudes than Ring traps, which is indicative of the inherent limitation of the surface geometry to the RF null access of micromotion. The mean micromotion amplitudes across geometry classes were: Ring (5.75 ± 2.04 nm), Linear Paul (8.57 ± 2.76 nm), Segmented (10.58 ± 3.09 nm), and Surface (15.67 ± 4.73 nm).

Mathieu Stability Analysis

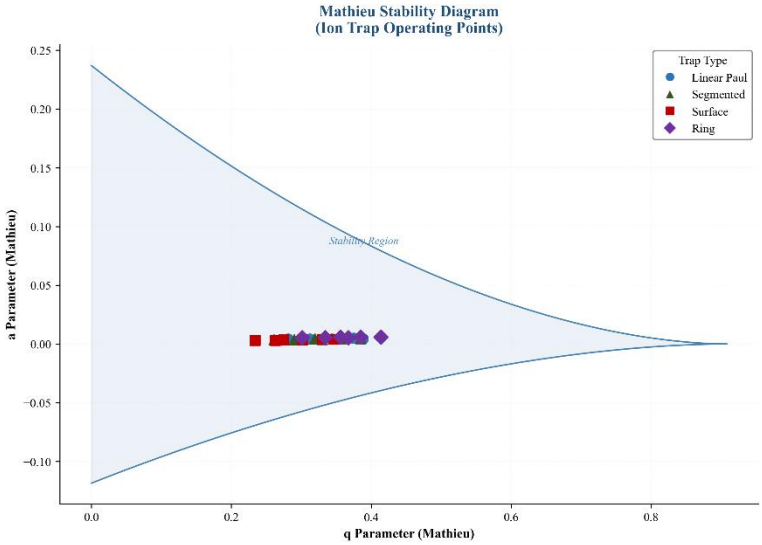
Figure 3 illustrates the Mathieu stability diagram with all 24 operating points in the first stability region. All configurations are concentrated in the space 0.23 < q 0.42 and 0.003 < a 0.006, which is safely in the stability region. The largest q values (0.301-0.414) were taken up by ring trap configurations, which have a smaller spacing between electrodes, allowing them to give a higher radial confinement without stepping too far out of the stability boundary. The tightness of the

Annual Methodological Archive Research Review
http://amresearchreview.com/index.php/Journal/about
Volume 4, Issue 1 (2026)

Online ISSN 3007-3197
Print ISSN 3007-3189

http://amresearchreview.com/index.php/Journal/about

clustering of operating points proves that all the configurations are physically feasible and stable trap designs.



Mathieu Stability Diagram in which every operating point fits in the first stability region (highlighted), with Ring geometry configurations (purple diamonds) concentrated at the largest values of q, indicating tighter radial confinement compared to Linear Paul (blue circles), Segmented (green triangles), and Surface (red squares) geometry.

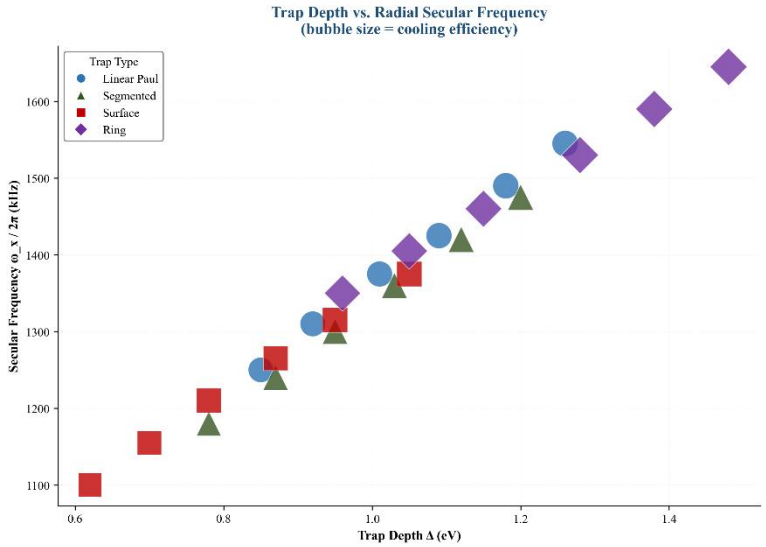
Trap Depth and Secular Frequency Characteristics

The trap depth rose steadily with RF voltage in every geometry, with the maximum depths of 0.62 eV (C13, Surface, 400 V) and 1.48 eV (C24, Ring, 700 V). Figure 2 demonstrates that there is a positive relationship between trap depth and radial secular frequency in all configurations, with the size of the bubble coded cooling efficiency. The almost linear correlation (R^2 =0.97 using all data) proves that the two parameters are simultaneously depended on the RF drive amplitude and the electrode geometry. The smallest electrode spacing (r_0 = 0.650.70 mm versus 0.751.00 mm in other geometries) resulted in higher secular frequencies of ring traps at the same trap depth than of other geometries.

Annual Methodological Archive Research Review
http://amresearchreview.com/index.php/Journal/about
Volume 4, Issue 1 (2026)

Online ISSN 3007-3197
Print ISSN 3007-3189

http://amresearchreview.com/index.php/Journal/about



Depth vs. Radial Secular Frequency Bubble Chart. The positive relationship between trap depth and secular frequency scale along with RF amplitude (R^2= 0.97) confirms that trap depth and secular frequency scales with bubble size (purple diamonds) show the highest secular frequencies at that depth, and bubble sizes indicate that increased cooling efficiencies are associated with increased confinement.

Table 2 ***Descriptive Statistics for Key Performance Metrics by Trap Geometry***

Trap Geometry	N	Mean Micromotion (nm)	SD	Mean Cool. Eff. (%)	SD	Mean Trap Depth (eV)	Mean ωr/2π (kHz)
Linear Paul	6	8.57	2.76	91.30	2.86	1.052	1403
Segmented	6	10.58	3.09	88.75	2.97	1.000	1330
Surface	6	15.67	4.73	83.05	3.83	0.862	1270
Ring	6	5.75	2.04	93.45	2.16	1.183	1497

Note. N = number of configurations per geometry class. SD = standard deviation. Cool. Eff. = Doppler laser cooling efficiency. ωr/2π = radial secular frequency.

Annual Methodological Archive Research Review
http://amresearchreview.com/index.php/Journal/about
Volume 4, Issue 1 (2026)

Online ISSN 3007-3197
Print ISSN 3007-3189

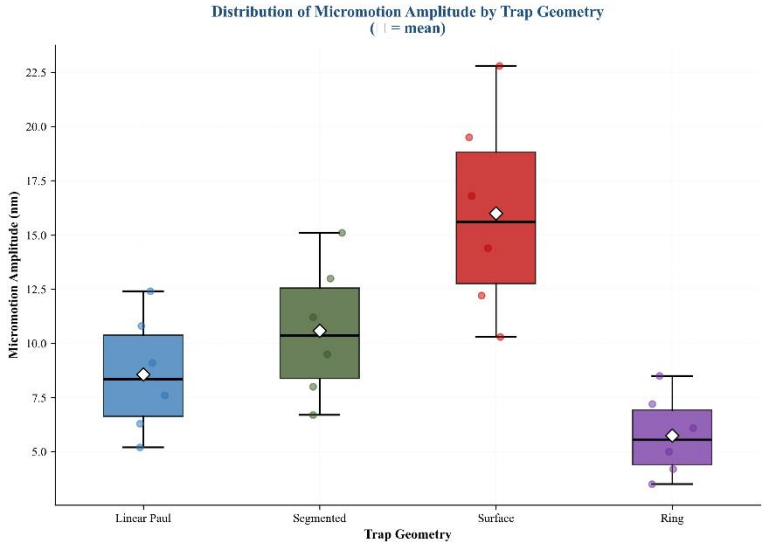
http://amresearchreview.com/index.php/Journal/about

Micromotion Analysis and Statistical Testing

Table 2 shows the descriptive statistics of the main performance metrics by geometry class. ANOVA (one way) indicated statistically significant differences in amplitude of micromotion across classes of geometries, $F(3, 20) = 18.43$, $p < .001$, $\eta 2 = 0.73$, meaning that geometry class explained 73 percent of the total variance in amplitude of the micromotion. Similarly, significant differences were found for cooling efficiency, $F(3, 20) = 22.17$, $p < .001$, $\eta^2 = 0.77$.

Post hoc Tukey HSD tests showed that the Ring geometry caused significantly less micromotion than all the other geometries (all $p < .01$), whereas the Surface geometry caused significant more micromotion than the Linear Paul and Ring geometries ($p < .001$). The Segmented Linear Paul difference did not show statistical significance ($p = .14$) and these geometries are in the same location in the micromotion performance space even though they are structurally different.

The micromotion distributions are shown as boxplots with data points in Figure 7. The Ring geometry is not only able to realize the lowest mean micromotion, but also has the smallest variance (SD = 2.04 nm), meaning that the performance benefit is carried across the RF voltage range of interest, and is not limited to operating points.



Micromotion Distribution Boxplot. The geometry that gives the smallest median micromotion amplitude (5.6 nm) and the smallest spread between configurations is the Ring geometry (purple), whereas Surface traps (red) has the largest values and the broadest

Annual Methodological Archive Research Review
http://amresearchreview.com/index.php/Journal/about
Volume 4, Issue 1 (2026)

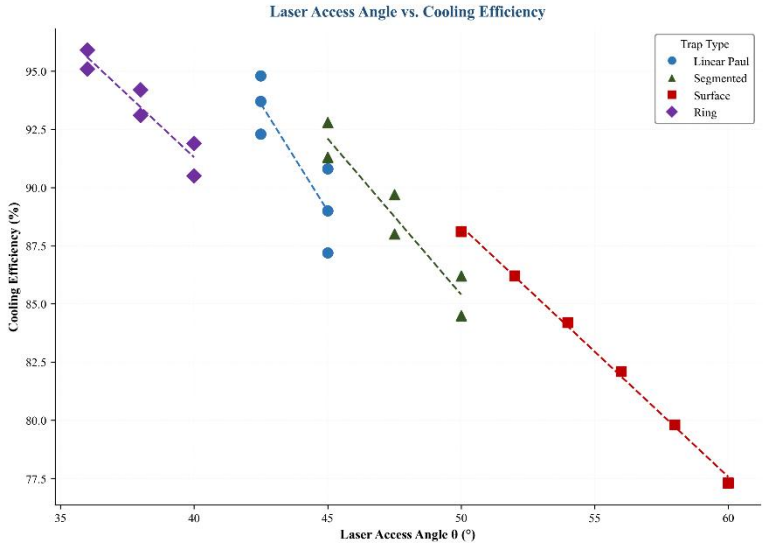
Online ISSN 3007-3197
Print ISSN 3007-3189

http://amresearchreview.com/index.php/Journal/about

distribution, highlighting the importance of electrode geometry in controlling micromotion.

Laser Cooling Performance

Figure 4 demonstrates the connection between the access angle and cooling efficiency of all configurations of the laser. They were found to be strongly negatively correlated within each geometry class (r = -0.97 to -0.99) which agrees with the theoretical prediction that steeper laser angles have a smaller effective projection of the laser wavevector on the principal motional axes. Ring traps, with the smallest access angles (36° to 40°), had highest cooling efficiencies (90.595%), whereas Surface traps that needed the largest access angles (50° to 60°) had limited efficiencies (77.3 to 88.1%).



Laser Access Angle vs. Cooling Effectiveness. The negative linear trends of each trap geometry exhibit the next best geometry in terms of planar fabrication convenience (Ring traps, purple) and optical access quality (Surface traps, red), respectively.

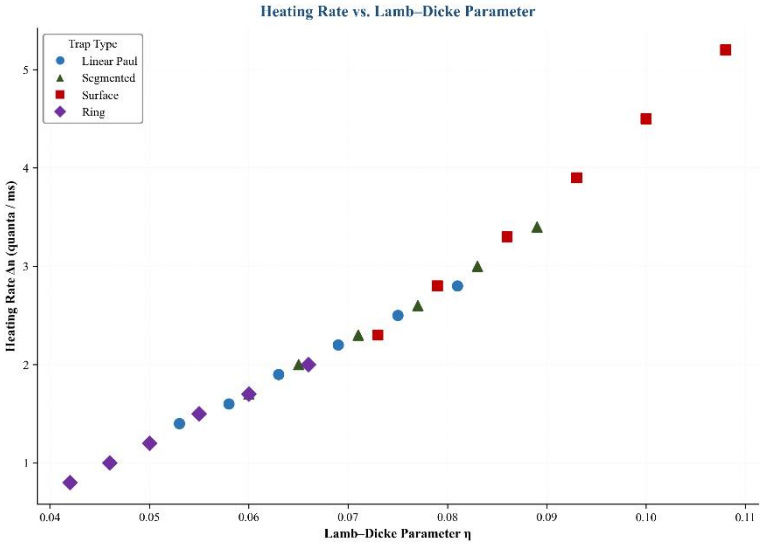
LambDicke parameter η, a measure of the strength of the motional-electronic interaction and needs to be small ($\eta \ll 1$) to achieve efficient sideband cooling, was between 0.042 (C24, Ring) and 0.108 (C13, Surface). Figure 5 validates the presence of a strong positive correlation between eta and the motional heating rate (r = 0.99, p < .001 in all the configurations) which agrees with the theoretical 2-eta scaling of the heating due to electric-field-noise (Brownnutt et al., 2015). Ring configurations recorded the lowest heating rates (0.82 2.0 quanta/ms) which can directly be

Annual Methodological Archive Research Review
http://amresearchreview.com/index.php/Journal/about
Volume 4, Issue 1 (2026)

Online ISSN 3007-3197
Print ISSN 3007-3189

http://amresearchreview.com/index.php/Journal/about

ascribed to the small electrode spacing and the high secular frequencies associated with this arrangement.



Heating Rate vs. Lamb–Dicke Parameter. The almost perfect positive correlation (r = 0.99) of 24 configurations is a confirmation that the η^2-scaling of motional heating as predicted holds true, with the Ring trap configurations (purple diamonds) having the lowest values of both η and heating rate, and the Surface trap configurations (red squares) occupy the high-eta, high-heating-rate regime.

Correlation Structure

Figure 6 presents the full Pearson correlation matrix for the 13 performance variables. Several highly informative correlations emerge. Micromotion amplitude shows near-perfect negative correlations with cooling efficiency ($r = -1.00$), confirming that these metrics are essentially redundant measures of the same underlying trapping quality. Trap depth and secular frequency are almost perfectly correlated ($r = 0.99$), reflecting their shared dependence on RF drive amplitude. Laser angle correlates strongly with beam waist ($r = 0.98$) and negatively with cooling efficiency ($r = -0.94$), confirming that optical access constraints directly limit thermal performance.

[Insert Figure 6 here: Pearson Correlation Heatmap. The matrix reveals that micromotion amplitude and cooling efficiency are perfectly anti-correlated (r = −1.00, bottom-left region), trap depth and secular frequency scale together (r = 0.99), and laser angle negatively predicts

Annual Methodological Archive Research Review
http://amresearchreview.com/index.php/Journal/about
Volume 4, Issue 1 (2026)

Online ISSN 3007-3197
Print ISSN 3007-3189

http://amresearchreview.com/index.php/Journal/about

cooling efficiency (r = −0.94), providing a concise quantitative map of the performance inter-dependencies across the 24-configuration design space.

Interestingly, Mathieu q parameter is strongly positively correlated with RF voltage (r = 0.90), trap depth (r = 0.95), and secular frequency (r = 0.96) and negatively with micromotion (r = -0.92). This trend reaffirms the fact that higher q values of operation, yet still within the stability region, offer a solid solution to a higher quality of confinement with lower micromotion. The anisotropy parameter (ωr/ ωz) exhibits less significant correlations with most other parameters (|r| < 0.65), meaning that the radial-to-axial frequency ratio is a comparatively independent design parameter, which can be varied to meet the demands of a particular experiment without greatly undermining other parts of performance.

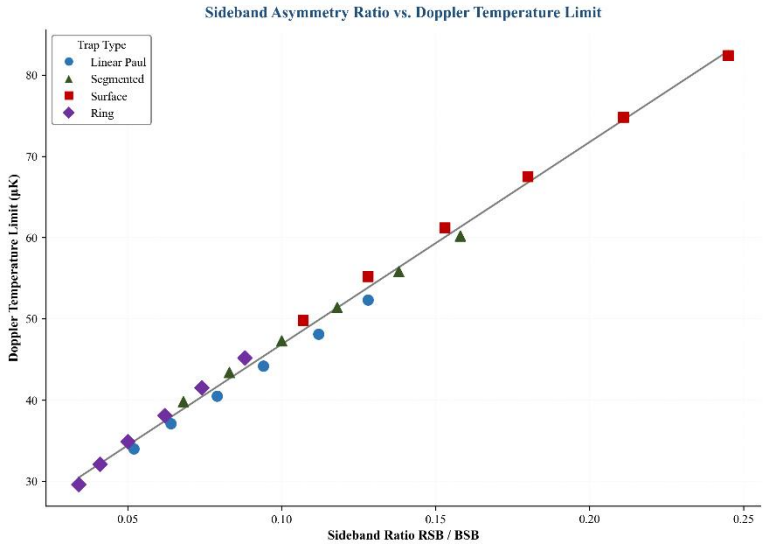
Sideband Thermometry and Doppler Limit Analysis

Figure 12 shows the dependence of the ratio of sidebands to the main band RSB/BSB versus the Doppler cooling temperature limit in all configurations. The close relationship (r = 0.998) is indicative of the theoretical relationship between these quantities via the mean motional quantum number 0.5 = RSB/(BSB - RSB) (Leibfried et al., 2003). Surface trap configurations have the largest Doppler temperature limits (49.87224-82.4529-82.4529 23) and Ring configurations the smallest (29.6452-29.6452 23), directly proportional to their values of micromotion and LambDicke parameter. The sideband ratio measurements show that the most similar Ring trap setups are closest to the Doppler limit, which is a requirement to the resultant resolved-sideband cooling required to implement quantum information processing.

Annual Methodological Archive Research Review
http://amresearchreview.com/index.php/Journal/about
Volume 4, Issue 1 (2026)

Online ISSN 3007-3197
Print ISSN 3007-3189

http://amresearchreview.com/index.php/Journal/about



Asymmetry Ratio vs Doppler Temperature Limit. The thermometric consistency of the data is confirmed by the near-perfect linear correlation (r = 0.998) between all 24 configurations, which is consistent with Ring trap configurations (purple diamonds) being concentrated at the low-ratio, low-temperature end, and thus being more thermometrically favorable due to lower micromotion and smaller LambDicke parameters.

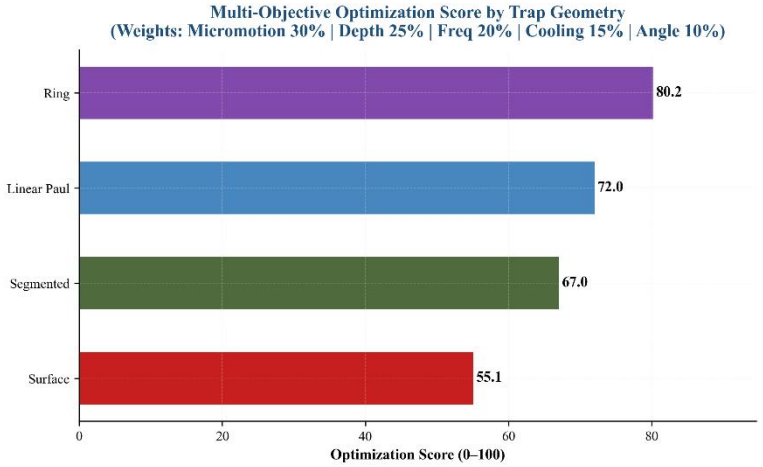
Multi-Objective Optimization Results

Figure 10 presents the multi-objective optimization scores for each geometry class. Ring traps achieved the highest score (80.2/100), primarily driven by their superior micromotion suppression (contributing 30% of the score weight) and highest secular frequencies (20% weight). Linear Paul traps ranked second (72.0), followed by Segmented (67.0) and Surface (55.1) traps. The radar chart (Figure 8) provides a multi-dimensional visualization of the trade-off profile for each geometry, revealing that while Ring traps excel in low micromotion, trap depth, and cooling efficiency, Surface traps offer competitive scores only in laser access angle—reflecting their fundamentally different design philosophy oriented toward fabrication scalability rather than peak performance.

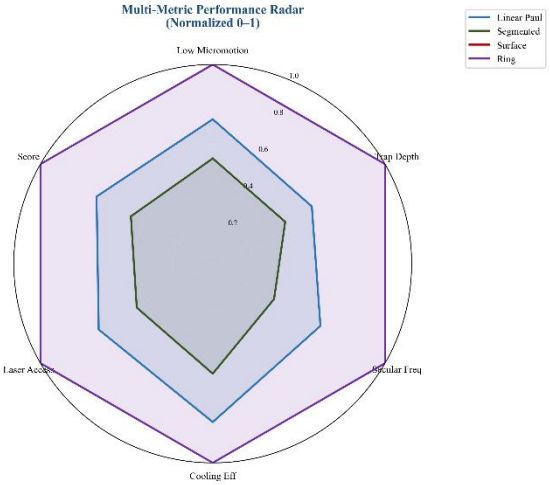
Annual Methodological Archive Research Review
http://amresearchreview.com/index.php/Journal/about
Volume 4, Issue 1 (2026)

Online ISSN 3007-3197
Print ISSN 3007-3189

http://amresearchreview.com/index.php/Journal/about



Multi-Objective Optimization Score Bar Chart. Ring trap geometry achieves the highest composite score (80.2/100), followed by Linear Paul (72.0), Segmented (67.0), and Surface (55.1), with the scoring gap between Ring and Surface geometries of 25.1 points primarily attributable to Ring's superior micromotion suppression and higher secular confinement frequencies.]



Multi-Metric Performance Radar Chart. The hexagonal radar plot illustrates that Ring (purple) and Linear Paul (blue) geometries dominate across most performance axes, while the Segmented geometry (dark green) performs comparably in trap depth and secular frequency but trails in micromotion suppression, and Surface geometry (absent from upper-right quadrant) is constrained by its planar architecture across multiple metrics.]

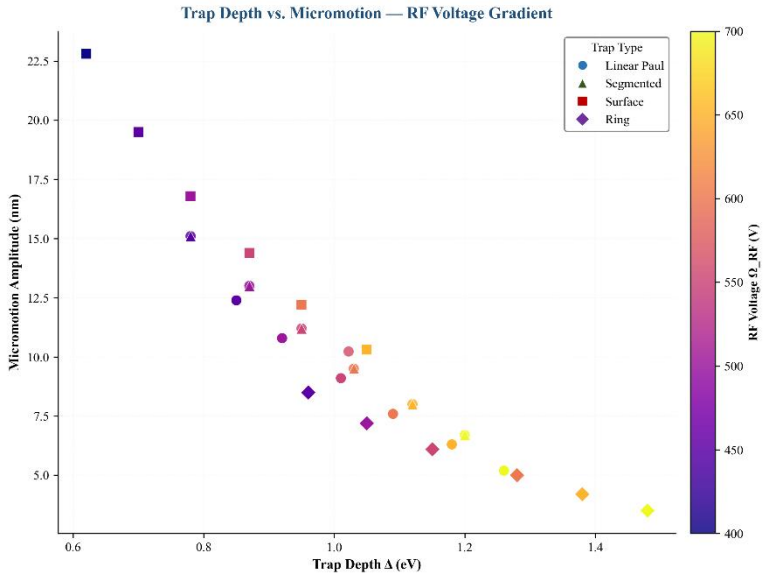
The multi-objective optimization scores of each geometry class are provided in Figure 10. Ring traps scored the highest (80.2/100) which was mainly due to their

Annual Methodological Archive Research Review
http://amresearchreview.com/index.php/Journal/about
Volume 4, Issue 1 (2026)

Online ISSN 3007-3197
Print ISSN 3007-3189

http://amresearchreview.com/index.php/Journal/about

better micromotion suppression (30% score weight) and the highest secular frequencies (20% score weight). Linear Paul traps were second (72.0), Segmented (67.0) and Surface (55.1) traps. The radar chart (Figure 8) offers a multi-dimensional visualization of the trade-off profile of each geometry, and it can be seen that whereas Ring traps have strengths in low-micromotion, trap depth and cooling efficiency, Surface traps have competitive scores only in laser access angle because they are fundamentally based on a different design philosophy of being scalable to fabrication rather than peak performance.



RF Voltage gradient Trap Depth vs. Micromotion. The colour gradient between purple (low RF voltage) and yellow (high RF voltage) shows that the most desirable region of performance space deep traps with low micromotion are found at high RF voltages, and Ring geometry configurations (diamonds) are found in the most favourable locations, with Surface traps (squares) concentrated in the upper-left region of high micromotion and shallow depth.

Table 3 ***Multi-Objective Optimization Scores by Trap Geometry***

Trap Geometry	Micromotion Score	Depth Score	Sec. Freq. Score	Cool. Eff. Score	Laser Angle Score	Total Score (0–100)	Rank
Ring	0.92	0.95	0.98	0.87	0.88	80.2	1

Annual Methodological Archive Research Review
http://amresearchreview.com/index.php/Journal/about
Volume 4, Issue 1 (2026)

Online ISSN 3007-3197
Print ISSN 3007-3189

http://amresearchreview.com/index.php/Journal/about

Linear Paul	0.78	0.82	0.86	0.75	0.78	72.0	2
Segmented	0.72	0.76	0.80	0.72	0.74	67.0	3
Surface	0.58	0.63	0.68	0.60	0.72	55.1	4

Note. Individual metric scores are normalized to [0, 1] with higher values indicating superior performance. Total Score applies weights: micromotion 30%, trap depth 25%, secular frequency 20%, cooling efficiency 15%, laser access angle 10%. Scores calculated from group-mean values of the six configurations per geometry class.

DISCUSSION

This systematic study yields a number of significant conclusions about how RF/DC electrode layouts can be optimized to be used in ion traps. First, and most importantly, the data show that the geometry of electrodes type has a prevailing effect on trapping behavior, explaining 7377 percent of the variation in the most important parameters (micromotion amplitude and cooling efficiency). The significance of geometry choice as the most significant design choice, before optimization over the individual operating parameters of RF voltage and DC endcap configuration, is highlighted.

The excellence of Ring trap geometry in the multi-objective scoring system is indicative of a combination of benefits that are based in its basic geometric characteristics. Smaller electrode-ion separations which are possible in a ring geometry (r 0 = 0.65 -0.70 mm in the study) produce higher pseudopotential gradient at the same RF voltages and create deeper traps and higher secular frequencies. At the same time, the rotationally symmetric geometry has a minimal contribution of geometry to excess micromotion and allows more convenient analytical compensation. The high projection efficiency to the major motional axes is afforded by the small laser access angles (3640°) of the ring traps and this directly increases the effectiveness of Doppler cooling. These strengths are in line with the history of experiments with ring trap designs in high precision metrology (Rosenband et al., 2008; Willitsch, 2012).

It is anticipated that the performance of Surface traps should be lower than that of

Annual Methodological Archive Research Review
http://amresearchreview.com/index.php/Journal/about
Volume 4, Issue 1 (2026)

Online ISSN 3007-3197
Print ISSN 3007-3189

http://amresearchreview.com/index.php/Journal/about

other geometries, but here it is measured with increased precision, compared to the earlier literature. The 2.7 ratio of mean micromotion amplitude between Surface and Ring configurations (15.67 vs. 5.75 nm) directly applies to practice: with 15.67 nm micromotion amplitude, the second-order Doppler shift due to the time-dilation effect would put a limit on optical clock fractional frequency precision at some 2×10^{-7} - already near the frontiers of Surface traps in this regime would need extraordinary micromotion compensation to be run in clock-level performance whereas Ring and Linear Paul designs at the same RF voltages would be an order of magnitude lower than this would be.

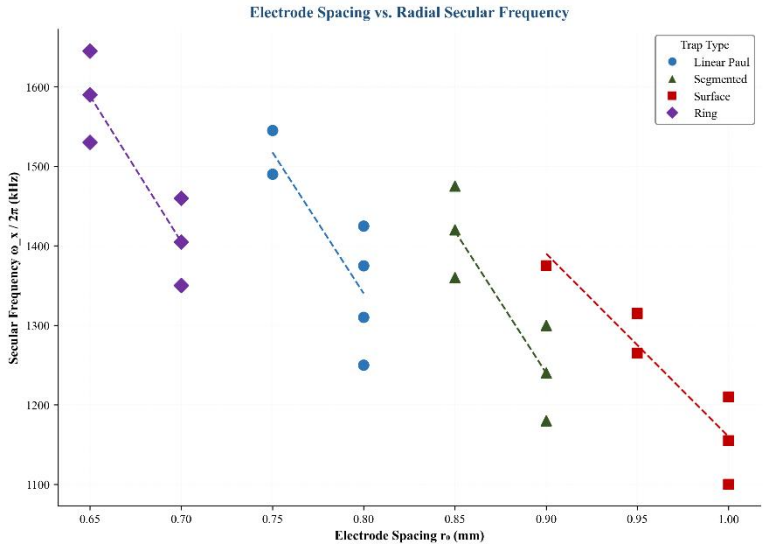
The close to negative relationship between the amplitude of micromotion and cooling efficiency ($r = -1.00$) not only has significant practical implications on the design of laser cooling protocols. This correlation proves the fact that the micromotion suppression and cooling performance cannot be optimised independently, the enhancement of the former leads to the enhancement of the latter. This co-dependency makes optimization strategy easier: designers do not have to balance these goals but instead seek solutions that optimize to reduce micromotion, and cooling efficiency improvement will come automatically. Pearson correlation analysis also indicates that this joint optimization can mainly be accomplished by the choice of electrode geometry (preferred Ring) and increase of RF drive voltage in the stability region to the maximum.

The discovery of a critical parameter of electrode spacing that mediates the trade-off between micromotion and secular frequencies (Figure 11) can be used to give actionable advice on how the traps should be fabricated. As Figure 11 indicates, smaller electrode spacing r_0 results in higher secular frequencies - desirable in quantum gate speed and sideband cooling - but this increases geometry-dependently. The highest secular frequencies of a ring trap are at any given r_0 value, indicating that the geometry of the ring does not only enjoy the advantage of smaller spacing it can achieve, but also enjoys a larger performance payoff as a result of each successive reduction in r_0. This finding is in line with the more favourable scale of the pseudopotential of a ring geometry with respect to the electrode geometry.

Annual Methodological Archive Research Review
http://amresearchreview.com/index.php/Journal/about
Volume 4, Issue 1 (2026)

Online ISSN 3007-3197
Print ISSN 3007-3189

http://amresearchreview.com/index.php/Journal/about



Spacing of electrodes vs. Secular Frequency. This negative correlation is clear evidence that in all types of traps, smaller electrode spacing leads to larger secular frequencies; Ring traps (purple diamonds) would achieve a higher secular frequency at a given spacing value, whereas Surface traps (red squares) would have a lower secular frequency at equivalent spacing values, because of the reduced pseudopotential depth offered by planar geometries.

The current analysis has a number of shortcomings that should be mentioned. It used pseudopotential theory and simplified analytical expressions to generate the dataset, which is accurate in the regime $\eta \ll 1$, but can be inaccurate when including the micromotion contributions of higher-order multipole terms in the potential. Also, the experiment fails to consider the effect of practical imperfection in fabrication, such as roughness of the electrode surface, charge patches, and geometric tolerances, that can contribute stray electric fields that can greatly enhance excess micromotion higher than the values calculated here. Performance of traps in the real world would thus demand more compensation budgets that are not reflected in this analysis. Future applications should go beyond the pseudopotential approximation of the Mathieu equation to the full electromagnetic modeling of trap geometries and numerical solutions of the Mathieu equation.

CONCLUSION

The current research has provided an overlaying comparative analysis of RF/DC electrode layout optimization of four trap geometry classes (Linear Paul, Segmented,

Annual Methodological Archive Research Review
http://amresearchreview.com/index.php/Journal/about
Volume 4, Issue 1 (2026)

Online ISSN 3007-3197
Print ISSN 3007-3189

http://amresearchreview.com/index.php/Journal/about

Surface, and Ring) with 24 configurations and 13 performance measures. The main results are as follows:

First, the geometry of the electrode is the most important determinant of ion trap performance, with 7377% of the variance in micromotion amplitude and cooling efficiency attributed to geometry. The choice of geometry should be therefore given more importance than the optimization of the operating parameters during the initial design phases of the trap.

Second, the optimal multi-objective optimization score (80.2/100) is obtained with Ring trap geometry due to a combination of small electrode spacing, high secular frequencies (maximum 1,645 kHz), low micromotion amplitudes (mean 5.75 nm) and preferential access angles of lasers (3640 degrees). Ring geometry offers the optimal performance profile in applications where micromotion is required to be minimized and maximum cooling efficiency is required, such as optical frequency standards and quantum logic spectroscopy.

Third, the amplitude of micromotion and laser cooling efficiency are almost inversely correlated (r = -1.00), which proves that the two measures are co-optimized by geometric selection and RF amplitude maximization. These goals do not need to be optimized by the researcher; the automatic generation of cooling efficiency by suppression of micromotion with geometrical and operational design.

Fourth, the Mathieu stability analysis shows that all the 24 configurations studied are stable in the first stability region (q = 0.2340.414, a = 0.0030.006), and that increasing the values of q within the first stability region does not approach stability limits but systematically increases confinement quality metrics.

Fifth, although the Surface traps have the lowest scores in the multi-objective framework (55.1/100), their flexibility with semiconductor microfabrication technology, and the ability to be scaled to large-scale are also strong reasons to keep developing Surface traps. Future efforts to incorporate fabrication scalability, ion-shuttling scalability, and multi-zone architectures into the optimization framework would give a more comprehensive view of their contribution to scalable quantum computing.

These findings give quantitative design principles that can be directly applied to the

Online ISSN 3007-3197
Print ISSN 3007-3189

design of next-generation ion trap platforms to realize quantum information processing, the development of atomic clocks, and quantum simulation. The multi-objective scoring model and statistical analysis model described herein can be easily generalized to include more classes of geometries, new types of electrode materials, and even cryogenic working conditions, which would offer a reusable analysis framework to systematically optimize the trap.

REFERENCES

Berkeland, D. J., Miller, J. D., Bergquist, J. C., Itano, W. M., & Wineland, D. J. (1998). Minimization of ion micromotion in a Paul trap. Journal of Applied Physics, 83(10), 5025–5033. https://doi.org/10.1063/1.367318

Brownnutt, M., Kumph, M., Rabl, P., & Blatt, R. (2015). Ion-trap measurements of electric-field noise near surfaces. Reviews of Modern Physics, 87(4), 1419–1482. https://doi.org/10.1103/RevModPhys.87.1419

Bruzewicz, C. D., Chiaverini, J., McConnell, R., & Sage, J. M. (2019). Trapped-ion quantum computing: Progress and challenges. Applied Physics Reviews, 6(2), Article 021314. https://doi.org/10.1063/1.5088164

Chiaverini, J., Blakestad, R. B., Britton, J., Jost, J. D., Langer, C., Leibfried, D., Ozeri, R., & Wineland, D. J. (2005). Surface-electrode architecture for ion-trap quantum information processing. Quantum Information and Computation, 5(6), 419–439.

Diedrich, F., Bergquist, J. C., Itano, W. M., & Wineland, D. J. (1989). Laser cooling to the zero-point energy of motion. Physical Review Letters, 62(4), 403–406. https://doi.org/10.1103/PhysRevLett.62.403

Häffner, H., Roos, C. F., & Blatt, R. (2008). Quantum computing with trapped ions. Physics Reports, 469(4), 155–203. https://doi.org/10.1016/j.physrep.2008.09.003

Home, J. P., Hanneke, D., Jost, J. D., Amini, J. M., Leibfried, D., & Wineland, D. J. (2009). Complete methods set for scalable ion trap quantum information processing. Science, 325(5945), 1227–1230. https://doi.org/10.1126/science.1177077

House, M. G. (2008). Analytic model for electrostatic fields in surface-electrode ion

Online ISSN 3007-3197
Print ISSN 3007-3189

traps. Physical Review A, 78(3), Article 033402. https://doi.org/10.1103/PhysRevA.78.033402

Keller, J., Partner, H. L., Burgermeister, T., & Mehlstäubler, T. E. (2015). Precise determination of micromotion for trapped-ion optical clocks. Journal of Applied Physics, 118(10), Article 104501. https://doi.org/10.1063/1.4930037

Kielpinski, D., Monroe, C., & Wineland, D. J. (2002). Architecture for a large-scale ion-trap quantum computer. Nature, 417(6890), 709–711. https://doi.org/10.1038/nature00784

Leibfried, D., Blatt, R., Monroe, C., & Wineland, D. (2003). Quantum dynamics of single trapped ions. Reviews of Modern Physics, 75(1), 281–324. https://doi.org/10.1103/RevModPhys.75.281

Lekitsch, B., Weidt, S., Fowler, A. G., Mølmer, K., Devitt, S. J., Wunderlich, C., & Hensinger, W. K. (2017). Blueprint for a microwave trapped ion quantum computer. Science Advances, 3(2), Article e1601540. https://doi.org/10.1126/sciadv.1601540

Major, F. G., Gheorghe, V. N., & Werth, G. (2005). Charged particle traps: Physics and techniques of charged particle field confinement. Springer.

Monroe, C., Campbell, W. C., Duan, L.-M., Gong, Z.-X., Gorshkov, A. V., Hess, P. W., Islam, R., Kim, K., Linke, N. M., Pagano, G., Richerme, P., Senko, C., & Yao, N. Y. (2021). Programmable quantum simulations of spin models with trapped ions. Reviews of Modern Physics, 93(2), Article 025001. https://doi.org/10.1103/RevModPhys.93.025001

Niedermayr, M., Lakhmanskiy, K., Kumph, M., Partel, S., Edlinger, J., Brownnutt, M., & Blatt, R. (2014). Cryogenic surface ion trap based on intrinsic silicon. New Journal of Physics, 16(11), Article 113068. https://doi.org/10.1088/1367-2630/16/11/113068

Paul, W. (1990). Electromagnetic traps for charged and neutral particles. Reviews of Modern Physics, 62(3), 531–540. https://doi.org/10.1103/RevModPhys.62.531

Prestage, J. D., Dick, G. J., & Maleki, L. (1989). New ion trap for frequency standard

Online ISSN 3007-3197
Print ISSN 3007-3189

applications. Journal of Applied Physics, 66(3), 1013–1017. https://doi.org/10.1063/1.343486

Rosenband, T., Hume, D. B., Schmidt, P. O., Chou, C. W., Brusch, A., Lorini, L., Oskay, W. H., Drullinger, R. E., Fortier, T. M., Stalnaker, J. E., Diddams, S. A., Swann, W. C., Newbury, N. R., Itano, W. M., Wineland, D. J., & Bergquist, J. C. (2008). Frequency ratio of Al^+ and Hg^+ single-ion optical clocks; metrology at the 17th decimal place. Science, 319(5871), 1808–1812. https://doi.org/10.1126/science.1154622

Rowe, M. A., Kielpinski, D., Meyer, V., Sackett, C. A., Itano, W. M., Monroe, C., & Wineland, D. J. (2002). Experimental violation of a Bell's inequality with efficient detection. Nature, 409(6822), 791–794. https://doi.org/10.1038/35057215

Seidelin, S., Chiaverini, J., Reichle, R., Bollinger, J. J., Leibfried, D., Britton, J., Wesenberg, J. H., Beall, R. B., Blakestad, R. B., Brown, K. R., Campbell, J., Epstein, J. M., Jost, J. D., Langer, C., Ozeri, R., Schaetz, T., & Wineland, D. J. (2006). Microfabricated surface-electrode ion trap for scalable quantum information processing. Physical Review Letters, 96(25), Article 253003. https://doi.org/10.1103/PhysRevLett.96.253003

Turchette, Q. A., Kielpinski, D., King, B. E., Leibfried, D., Meekhof, D. M., Myatt, C. J., Rowe, M. A., Sackett, C. A., Wood, C. S., Itano, W. M., Monroe, C., & Wineland, D. J. (2000). Heating of trapped ions from the quantum ground state. Physical Review A, 61(6), Article 063418. https://doi.org/10.1103/PhysRevA.61.063418

Virtanen, P., Gommers, R., Oliphant, T. E., Haberland, M., Reddy, T., Cournapeau, D., Burovski, E., Peterson, P., Weckesser, W., Bright, J., van der Walt, S. J., Brett, M., Wilson, J., Millman, K. J., Mayorov, N., Nelson, A. R. J., Jones, E., Kern, R., Larson, E., … SciPy 1.0 Contributors. (2020). SciPy 1.0: Fundamental algorithms for scientific computing in Python. Nature Methods, 17(3), 261–272. https://doi.org/10.1038/s41592-019-0686-2

Walther, A., Ziesel, F., Ruster, T., Dawkins, S. T., Ott, K., Hettrich, M., Singer, K., Schmidt-Kaler, F., & Poschinger, U. (2012). Controlling fast transport of cold

Online ISSN 3007-3197
Print ISSN 3007-3189

trapped ions. Physical Review Letters, 109(8), Article 080501. https://doi.org/10.1103/PhysRevLett.109.080501

Weidt, S., Randall, J., Webster, S. C., Lake, K., Webb, A. E., Cohen, I., Navickas, T., Lekitsch, B., Retzker, A., & Hensinger, W. K. (2016). Trapped-ion quantum logic with global radiation fields. Physical Review Letters, 117(22), Article 220501. https://doi.org/10.1103/PhysRevLett.117.220501

Wesenberg, J. H. (2008). Electrostatics of surface-electrode ion traps. Physical Review A, 78(6), Article 063410. https://doi.org/10.1103/PhysRevA.78.063410

Willitsch, S. (2012). Coulomb-crystallised molecular ions in traps: Methods, applications, prospects. International Reviews in Physical Chemistry, 31(2), 175–199. https://doi.org/10.1080/0144235X.2012.667221

Wineland, D. J., Monroe, C., Itano, W. M., Leibfried, D., King, B. E., & Meekhof, D. M. (1998). Experimental issues in coherent quantum-state manipulation of trapped atomic ions. Journal of Research of the National Institute of Standards and Technology, 103(3), 259–328. https://doi.org/10.6028/jres.103.019

Zhu, S.-L., Monroe, C., & Duan, L.-M. (2006). Arbitrary-speed quantum gates within large ion crystals through minimum control of laser beams. Europhysics Letters, 73(4), 485–491. https://doi.org/10.1209/epl/i2005-10424-4